Spatiotemporal Variations in Grassland Desertification Based on Landsat Images and Spectral Mixture Analysis in Yanchi County of Ningxia, China

Jinya Li, Lina Zhao, Bin Xu, Xiuchun Yang, Yunxiang Jin, Tian Gao, Haida Yu, Fen Zhao, Hailong Ma, and Zhihao Qin

***Abstract*—Facing the worsening degradation of grasslands, state and local governments in China have implemented a series of ecological protection projects. Ningxia Hui Autonomous Region was the first province in China to implement a region-wide grazing ban, the effect of which has become contentious at all levels of government and a topic of public concern. The change of grassland desertification is the most direct indicator of the grazing ban's effect. This paper chooses Yanchi County in Ningxia as the study area to analyze the grassland desertification situation. Based on a series of Landsat TM/ETM+ images, field observations and expert review, a Ningxia grassland desertification classification and grading system was constructed. Then, spectral mixture analysis (SMA) and a decision-tree method were used to interpret images of the study area from 4 years: 1993, 2000, 2006, and 2011. The following results were obtained: the area of desertified grassland decreased gradually from 4142 km^2 in 1993 to 3695 km^2 in 2011, a decrease of 10.80%. The severity of desertification also declined as the area of severely desertified grassland gradually decreased to 324 km^2 in 2011 from 1093 km^2 in 1993, a decrease of 70.34%. The annual reduction rate of the desertified grassland area reached its peak during the period 2000–2006. In particular, the areas of severely desertified grassland declined by 8.86% annually. In a situation of declining rainfall, human factors (such as ecological protection policy) have become a major cause of ongoing grassland desertification reversal and restoration of grassland vegetation.**

***Index Terms*—Grassland desertification, grazing ban, remote sensing, spatiotemporal analysis, spectral mixture analysis (SMA).**

Manuscript received October 30, 2013; revised May 24, 2014; accepted July 30, 2014. This work was supported in part by the National Natural Science Foundation of China (NSFC) under Grant 31372354, in part by the International Science and Technology Cooperation Program of China under Grant 2013DFR30760, in part by Grassland Monitoring and Supervision Center Ministry of Agriculture, China under Grant 425-1, and in part by the Centre of Supervision Management of Grassland, Ministry of Agriculture, China. *(Corresponding author: Bin Xu.)*

J. Li is with the State Key Laboratory of Urban and Regional Ecology, Research Center for Eco-Environmental Sciences, Chinese Academy of Sciences, Beijing 100085, China, and also with the Key Laboratory of Agri-Informatics, Ministry of Agriculture, Institute of Agricultural Resources and Regional Planning, Chinese Academy of Agricultural Sciences, Beijing 100081, China (e-mail: jyli@rcees.ac.cn).

B. Xu is with the Key Laboratory of Agri-Informatics, Ministry of Agriculture, Institute of Agricultural Resources and Regional Planning, Chinese Academy of Agricultural Sciences, Beijing 100081, China (e-mail: xubin@caas.cn).

L. Zhao is with the Institute of Botany, Chinese Academy of Sciences, Beijing 100093, China (e-mail: zhaoln@ibcas.ac.cn).

X. Yang, Y. Jin, T. Gao, H. Yu, F. Zhao, H. Ma, and Z. Qin are with the Institute of Agricultural Resources and Regional Planning, Chinese Academy of Agricultural Sciences, Beijing 100081, China (e-mail: yangxiuchun@caas.cn; jinyunxiang@caas.cn; gaotianwuyi@163.com; yuhaida5920@163.com; zhaofen198931@163.com; mahailong@caas.cn; qinzhihao@caas.cn).

Color versions of one or more of the figures in this paper are available online at http://ieeexplore.ieee.org.

Digital Object Identifier 10.1109/JSTARS.2014.2348612

I. Introduction

DESERTIFICATION, meaning land degradation in arid, semiarid, and dry subhumid areas resulting from climatic variations and/or human activities [1], [2], is one of the most critical environmental hazards, and is also an important factor leading to poverty and hindering economic and socially sustainable development. Grassland desertification, the primary form of grassland degradation in China, is also known as grassland sandy desertification. China has nearly 400 million hectares of natural grasslands, representing 41.7% of its territory. However, 90% of China's available natural grasslands exhibit varying degrees of degradation, of which reduced vegetative coverage, desertification, salinization, and other characteristics of moderate or severe degradation account for half [3]. Grassland desertification is the result of interaction between natural and human factors. Natural factors are the basis and the background of desertification occurrence and development. On long time scales and large spatial scales, the evolution of the desertification is closely tied to global climate change, but at specific times and places, human activities can also influence the evolution of desertification, even inhibiting or reversing desertification processes through particular behaviors or measures based on understanding the occurrence and development of desertification [4].

In recent years, state and local governments in China have implemented a series of ecological protection and environmental engineering programs, including the Grain for Green Project, the Beijing–Tianjin Dust Storms Sources Control Project and the grazing ban, among other ecological engineering measures, and have achieved significant results, especially in the farming–pastoral ecotone of northern China and other ecologically fragile areas, where the ecological environment has been improved significantly [5]–[7].

The Ningxia Hui Autonomous Region, with an area of 51 800 km^2, is located primarily in arid and semiarid zones and is surrounded by the Tengger Desert, the Ulan Buh Desert, and the Mu Us Sandland in the west, north, and east, respectively; this region is also one of the most desertified provinces (regions) in China. Since Ningxia was chosen as a sand prevention and control demonstration region, the desertified area in Ningxia has been significantly reduced and the desertification process has been reversed due to the implementation over recent years of the Three-North Shelterbelt Forest Program, the Grain for Green Project, and a region-wide grazing ban, among other ecological engineering measures [8]–[10]. However, the harsh natural environment and underdeveloped economic conditions in Ningxia have made the sandy area's ecology extremely fragile. The trend of desertification, officially described as "overall reversal but partial deterioration," continues. Further development of the anti-desertification work, including consolidation and ongoing management of the desertification reversal zone, remains necessary. Consequently, we need to continually improve desertification monitoring methods and systems in order to provide a reliable basis for sand prevention work, gradually achieve common development of desertification monitoring and control [8].

This paper selects Yanchi County in the Ningxia Hui Autonomous Region as the study area to analyze the grassland desertification situation in Ningxia. Based on Landsat $\mathrm{TM/ETM+}$ remote sensing images, field observations and expert review, a Ningxia grassland desertification classification and grading system was constructed. Then, spectral mixture analysis (SMA) and a decision-tree method were selected to interpret remote sensing images of the study area in four periods. After the status and variation trends of the grassland desertification were obtained, the driving factors that affect grassland desertification were analyzed to better understand the consequences of the desertification prevention work.

II. Materials and Methods

A. Study Area

The study site is located in the east of Ningxia Hui Autonomous Region with a total area of $6774.32\ \mathrm{km}^2$, from longitude $106°30'\mathrm{E}$ to $107°41'\mathrm{E}$ and latitude $37°04'\mathrm{N}$ to $38°10'\mathrm{N}$ (Fig. 1), and is approximately 110 km long from north to south and 66 km wide from east to west. The location is a typical transition zone of climate, topography, vegetation, and resource utilization: from semiarid to arid zones in climate, from the Loess Plateau to the Ordos Mesa in topography, from typical steppe to desert in vegetation and from farming zone to pasture zone in resource utilization. The fragility and instability of the natural environment in the study area is a product of this geographical transition.

The southern part is the Loess Plateau District, while the northern part is hilly Ordos Mesa with gentle slope, at an average altitude of 1600 m. It has a temperate continental climate: a long winter and short summer, strong wind and dust occurring frequently in winter and spring, abundant sunshine, large temperature variation, strong evaporation but low rainfall, an average annual temperature of 8.7°C and annual precipitation of 250–350 mm that is mostly concentrated in July and August and decreases from south to north, specifically

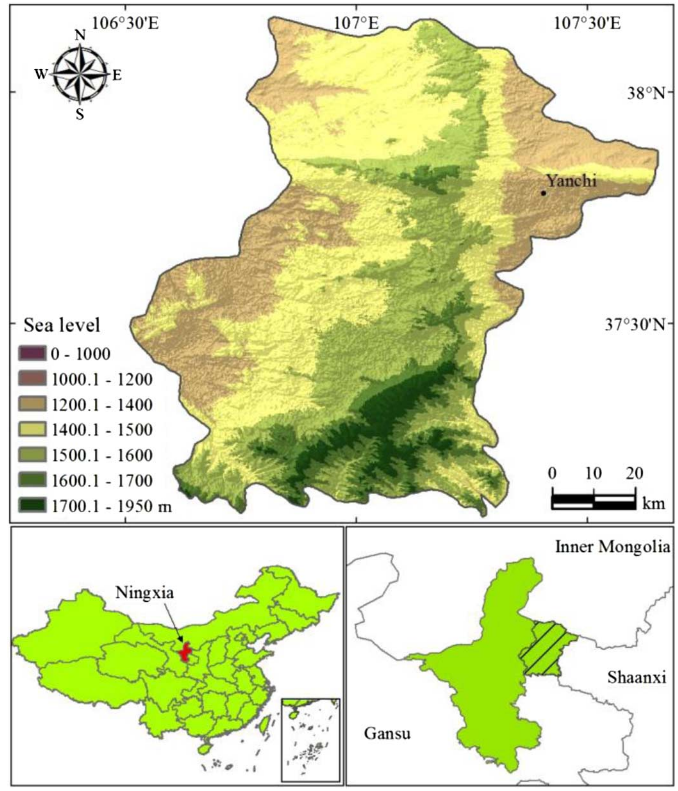

Fig. 1. Location of study area.

from southeast to northwest. The soil type in Yanchi County is mainly sierozem, followed by dark loessial soils and aeolian sandy soils, and the soil type is mainly aeolian sandy soils and sierozem with low organic matter content in the northern windy desert region. Grassland vegetation types are mainly typical steppe and temperate steppe desert.

B. Data Acquisition and Preprocessing

Landsat Thematic Mapper (TM5) and Landsat Enhanced Thematic Mapper plus $(\mathrm{ETM}+7)$ scenes acquired on June 16, 1993 (TM5 June 1993), August 30, 2000 $(\mathrm{ETM}+7$ August 2000) and August 7, 2006 (TM5 August 2006) were selected as they had similar levels of recent precipitation and were of good data quality (cloud free). Landsat images acquired on June 18, 2011 (TM5 June 2011) were selected to interpret the recent grassland desertification status, while the prior images were used to analyze the effect of the region-wide grazing ban that was implemented in 2003. With a resolution of 30 m, these time-series Landsat images (Path 129, Row 34) were acquired from June to September, during the region's typical growing season, and were downloaded from the United States Geological Survey (USGS) website (http://glovis.usgs.gov) at no cost. Geometric correction (root mean square error was less than one pixels) and atmospheric correction were performed on the selected Landsat $\mathrm{TM/ETM+}$ images using ENVI 4.8 (ITT Visual Solutions Inc.) according to the method described by Wang *et al.* [11] and Zhang *et al.* [12].

Other study area data, such as annual land-use mapping, meteorological data (rainfall and temperature), grassland type and soil type, were collected and collated. In addition, to

TABLE I
REMOTE SENSING GRADING SYSTEM OF GRASSLAND SANDY DESERTIFICATION IN YANCHI COUNTY

Grassland desertification intensity classification	Vegetation community characteristics		Bare-sand ratio (%)	Geomorphologic features
	Vegetation composition	Vegetation coverage (%)		
SlDG	Psammophytes become the main accompanying species	40–55	30–50	Relatively moderate sand, fixed sand dunes
MDG	Psammophytes become the dominant species	30–40	50–65	Moderate sand, small blowout pits or semi-fixed sand dunes
SeDG	Vegetation is very sparse, only a few psammophytes remaining	<30	>65	Medium and large sand dunes, large blowout pits, semi-mobile or mobile sand dunes

establish a grassland desertification classification system suitable to the study area and build the interpretation symbols preparing for visual interpretation, a field study of the research area was performed in July of 2012, during which extensive ground data were obtained that primarily consisted of spatial-location information, geomorphological features, sample plot and quadrat information, grazing and desertification conditions surrounding the sample plot and quadrat, and other ground data.

C. Grading System

Based on relevant desertification classification indicator studies [13]–[17], China's national standard "parameters for degradation, sandification, and salification of rangelands" (GB19377-2003) and field inspection and verification, combined with the land use, grassland type, and basic desertification characteristics of the study area, we classified the land cover of the study area into nine categories (shrubland was treated as grassland): 1) farmland; 2) forest; 3) human settlements; 4) water; 5) nondesertified grassland (nonDG); 6) slightly desertified grassland (SlDG); 7) moderately desertified grassland (MDG); 8) severely desertified grassland (SeDG), and others [18]. Finally, we conducted seminars and demonstration projects for experts to substantiate the scientific validity, operability, and interpretability of the remote sensing images. Combining the sample plots and quadrat data, the grassland type and general environment of the study area, we further determined the appropriate gradation system for remote sensing of grassland desertification in Ningxia (Table I).

D. Grassland Desertification Extraction Method

Traditional desertification information extraction methods can be divided into two main classes [19]: 1) calculation of vegetation indices and 2) image classification. The normalized difference vegetation index (NDVI) is a commonly used vegetation index to map temporal and spatial variation in vegetation. However, it is difficult to establish a direct relationship with grassland desertification and the index is vulnerable to soil background and other factors. NDVI has many limitations for desertification information extraction, often tending to overestimate the degree of desertification in sparsely vegetated areas [19]–[22]. Conventional visual interpretation and supervised classification, among other remote sensing interpretation methods, also have many limitations for desertification information extraction because of the difficulty of quantitative extraction or susceptibility to human subjectivity. The materials in a given pixel in remote sensing images are rarely represented by a single component, especially in arid and semiarid environments [19], [23]–[25]. SMA, as a subpixel classification method, has been promoted as an efficient method to derive coverage information from multispectral and hyperspectral imagery in arid and semiarid areas [23], [26], [27]. SMA is based on the concept that the relative proportion of a few spectrally distinct components is what dominates the variance across a given scene [23], [28]. SMA transforms radiation or reflectance data into fractions of a few dominant end-members, and the derivation of vegetation coverage and bare-sand ratios is the prerequisite basis for quantitative evaluation of grassland desertification. In this research, we selected the linear spectral mixture model (LSMM), one type of SMA that is widely used due to its simplicity, reasonable level of effectiveness and interpretability [19], [23], [29]–[31], as the main method to extract information on grassland desertification. In an LSMM, the reflectance of each pixel at each spectral band is considered as a linear combination of the reflectance of each end-member and its relative abundance [32] as follows

$$\rho(\lambda_i) = \sum_{j=1}^{m} F_j \rho_j(\lambda_i) + \varepsilon(\lambda_i) \tag{1}$$

where $j = 1, 2, \ldots, \mathrm{m}$ is the pixel component (end-member); $i = 1, 2, \ldots, \mathrm{n}$ is the spectral band; $\mathrm{m} \leq \mathrm{n} + 1$; $\rho(\lambda_i)$ is the reflectance of mixed pixels for each band (i); $\rho_j(\lambda_i)$ is the reflectance of the end-member j at band i; F_j refers to the abundance of the end-member j in the pixel (a parameter to be estimated); and $\varepsilon(\lambda_i)$ is the difference between the actual and modeled reflectance. F_j represents the best-fit coefficient that minimizes the root-mean-squared error *(RMSE)*

$$RMSE = \sqrt{(\sum_{i=1}^{n} \varepsilon^2(\lambda_i))/n} \tag{2}$$

where n is the number of bands and $\varepsilon(\lambda_i)$ is the residual term at band i ($i = 1, 2, \ldots, \mathrm{n}$).

The derived fractions of end-members are often subject to the unity constraint, which is derived as follows

$$\sum_{j=1}^{m} F_j = 1. \tag{3}$$

Appropriate and accurate end-member selection is crucial for the success of the LSMM. In this study, we conducted a

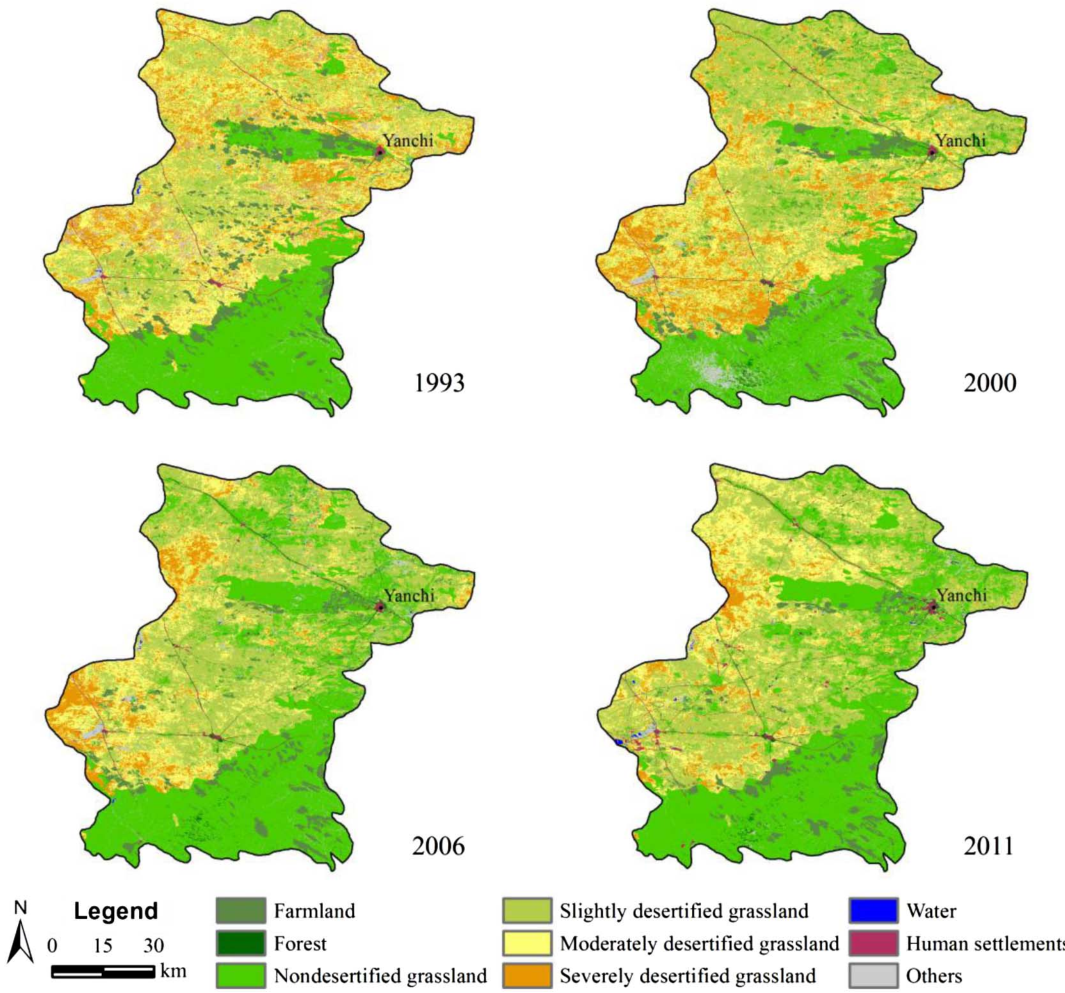

Fig. 2. Monitoring results of grassland sandy desertification of Yanchi County in four periods.

comprehensive field investigation to identify the optimal/most representative surface types and so find preferable locations for development of a spectral library from the Landsat images. Based on a field investigation, the $\mathrm{TM/ETM+}$ images were processed with a minimum noise fraction (MNF) rotation transformation; thus, the "pure" spectral end-members of vegetation, bare sand, and bare soil were extracted by iteratively testing different end-member combinations [33]–[36]. These end-members were then input into a spectral unmixing algorithm, thereby producing a bare sand fraction map and a vegetation coverage map.

Before producing unmixed pixels, a mask was made for farmland, human settlements, water, forest and other land uses based on visual interpretation, the normalized difference water index (NDWI) and the NDVI, among other methods. Then, the masked image was input into the LSMM, and a grading desertification map was made using the bare sand fraction map by decision-tree method according to the grading system (Table I). The classification accuracy was verified based on 300 random points that were identified by visual interpretation according to the interpretation symbols (based on field investigation) and land-use mapping as reference data. Then, the reference data and the classification result were compared and if the precision did not meet the requirements (greater than 80% accuracy), a different end-member combination would be tested [33]–[36].

III. Results and Discussion

A. Time Variation Characteristics

1) Statistical Characteristics: The classification maps obtained for four periods of monitoring Yanchi County grassland desertification are shown in Fig. 2, and the statistical results are shown in Table II. The results show that desertified grassland covered about 60% of the study area from 1993 to 2011 but it is in decline, decreasing by 10.80% from 4142 km^2 in 1993 to 3695 km^2 in 2011. The area of SlDG exhibited an increasing trend, from 1327 km^2 in 1993 to 2305 km^2 in 2011, representing an increase of 73.66%. The area of MDG and SeDG had an overall decreasing trend, especially the area of SeDG, which decreased significantly, from 1093 km^2 in 1993 to 324 km^2 in 2011, a decrease of 70.34%.

The gradual increase in SlDG area, the rapid decrease in SeDG area, and the decrease in total DG area indicate that the vegetation is in a state of recovery, and grassland desertification in Yanchi County has been reversed over the last

TABLE II
AREAS AND PROPORTIONS OF EACH MAJOR CLASS IN DIFFERENT PERIODS IN LING-YAN

Land types	1993		2000		2006		2011	
	Area (km^2)	Proportion (%)	Area (km^2)	Proportion (%)	Area (km^2)	Proportion (%)	Area (km^2)	Proportion (%)
SlDG	1327	19.59	1907	28.15	2298	33.93	2305	34.03
MDG	1722	25.42	1265	18.68	942	13.90	1066	15.73
SeDG	1093	16.13	999	14.75	468	6.91	324	4.79
Total DG	4142	61.14	4171	61.57	3708	54.74	3695	54.54
NonDG	1851	27.33	1850	27.30	2489	36.74	2544	37.55
Farmland	442	6.53	401	5.92	308	4.54	293	4.33
Forest	5	0.07	38	0.57	61	0.90	67	0.99
Water	3	0.04	0.4	0.01	2.6	0.04	6.7	0.10
Human settlements	38	0.57	44	0.65	43	0.64	80	1.18
Other	292	4.31	269	3.98	163	2.41	88	1.30

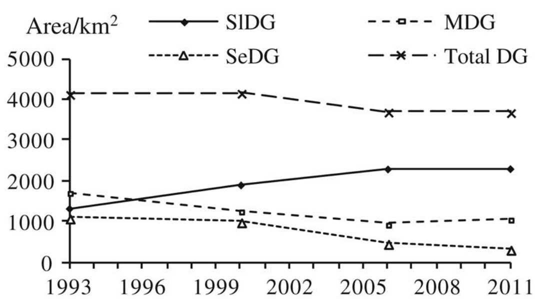

Fig. 3. Tendency chart of grassland desertification in Yanchi County from 1993 to 2011. SlDG, slightly desertified grassland; MDG, moderately desertified grassland; SeDG, severely desertified grassland; total DG, total desertified grassland.

two decades (Fig. 3). In particular, from 2000 to 2006, the SeDG and total DG areas decreased significantly. The SeDG area decreased from 999 km^2 in 2000 to 468 km^2 in 2006, a decrease of 53.14%, indicating that the region-wide grazing ban has played a significant role in the restoration of grassland vegetation in Yanchi County. The increasing trend of SlDG area flattened out after 2006, while the MDG area began to increase and the SeDG area continued decreasing, but at a reduced rate. The changes in trends suggest that the fragile ecological environment of the study area is quite susceptible to the impact of human factors. Banning of grazing and enclosure, among other anthropogenic interventions, are beneficial for the recovery of vegetation and the reversal of the desertification process.

2) Annual Rate: Through further processing of grassland desertification and other land-type data from various periods, an annual rate was obtained (Table III). The annual rates of SlDG growth for the three periods were 6.24%, 3.42%, and 0.06%; the fastest increase occurred before 2000 and the rate decelerated gradually thereafter. The annual rates of reduction in the MDG area were 3.79% and 4.26% during the two periods before 2006, and then these turned, with the area subsequently increasing by 2.63% annually. SeDG area showed a decreasing trend in all three periods, with higher reduction rates during the two periods after 2000, especially during the period 2000–2006, when the rate was as high as 8.86%, suggesting that the 2002 region-wide grazing ban and other ecological engineering measures played important roles in the rapid recovery of the vegetation and the reversal of the overall trend of grassland desertification.

B. Space Variation Characteristics

1) Statistical Characteristics: To demonstrate visually the variation of grassland desertification in degree and spatial distribution pattern, raster calculations as implemented in ArcGIS were used to obtain grassland desertification spatial distribution dynamic-change maps (Fig. 4) for 1993–2000, 2000–2006, and 2006–2011. We define the figure elements as follows: an increase in the degree of desertification from the previous period is termed "developed" desertification (e.g., a change from nonDG to SlDG); a cross-level increase in the desertification degree is termed "seriously developed" (e.g., a change from nonDG to MDG); a decrease in the degree of desertification is termed "reversed"; a cross-level decrease in the degree of desertification is termed "significantly reversed"; and no change in the degree of desertification between two periods is termed "stable" [6].

The statistical results of the spatial distribution dynamic change are shown in Table IV. The area of total developed (the combination of developed and seriously developed areas) during 1993–2000, 2000–2006, and 2006–2011 were 906 km^2, 578 km^2, and 985 km^2, respectively (13.38%, 8.54%, and 14.54% of the county area), while that of total reversed (the combination of reversed and significantly reversed areas) were 1492 km^2, 1964 km^2, and 1117 km^2, respectively (22.03%, 28.99%, and 16.49% of the county area). The differences in area between the total developed and total reversed desertification categories suggest that the overall trend of grassland desertification in Yanchi County is reversal; in particular, during the period 2000–2006, when the area gap between these two categories reached its peak, the area of total reversed was 3.40 times that of total developed, suggesting that the implementation of the region-wide grazing ban since 2002

This article has been accepted for inclusion in a future issue of this journal. Content is final as presented, with the exception of pagination.

TABLE III
ANNUAL CHANGE RATE OF EACH CLASS DURING VARIOUS PERIODS IN THE STUDY AREA

Period	SlDG	MDG	SeDG	Total DG	NonDG	Farmland	Forest	Water	Human settlements	Other
1993–2000	6.24	−3.79	−1.23	0.10	−0.01	−1.34	96.39	−12.35	2.20	−1.12
2000–2006	3.42	−4.26	−8.86	−1.85	5.76	−3.88	9.75	93.33	−0.45	−6.57
2006–2011	0.06	2.63	−6.15	−0.07	0.44	−0.92	2.14	30.91	17.08	−9.22

Positive values represent an increase and negative values represent a decrease. Unit: %.

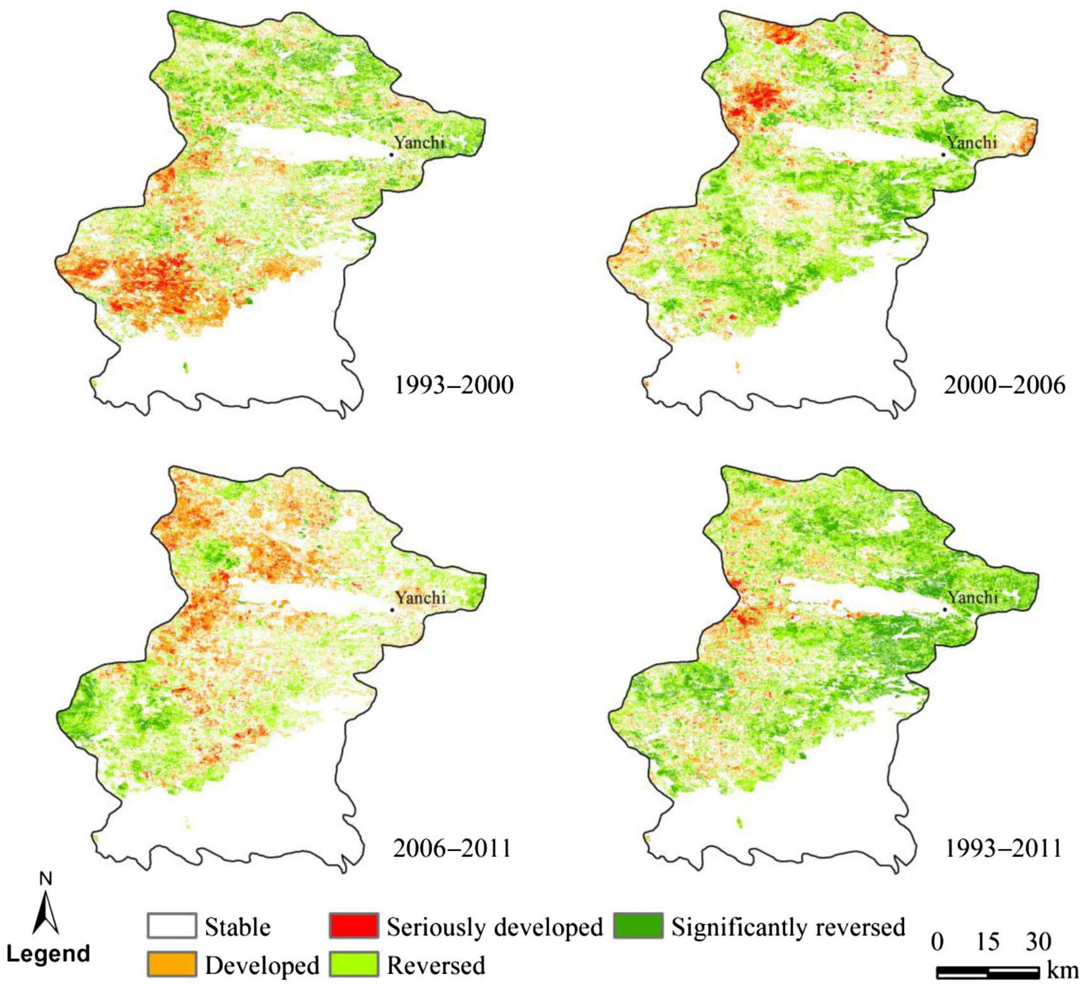

Fig. 4. Spatial distribution dynamic-change maps of grassland sandy desertification in Yanchi County.

has effectively promoted the recovery of the vegetation and lessened the degree of desertification in grassland. However, the gap narrowed during the period 2006–2011, suggesting that, after a certain period of recovery, grassland desertification passes through a fast reversal period, and the reversion and development of desertification approach an equilibrium state, in which the stability of the environment may be low and external forces may have important impacts on grassland desertification change direction.

2) Dynamic-Change Intensity: To demonstrate visually the spatial distribution dynamic-change intensity of grassland desertification, the data in Table IV were used to plot a tendency chart of grassland desertification spatial distribution dynamic-change intensity (Fig. 5). Annual changes in the reversed, significantly reversed and total reversed areas all show a pattern of increase followed by decrease, with both the area of reversed and total reversed being large for any given year. In contrast, annual changes in the developed, seriously developed, and total developed areas are all in the opposite direction and at a lower level. Neither of the two extreme change types, i.e., "seriously developed" and "significantly reversed," affects a large area. The "reversed" and "developed" change types primarily set the trends in spatial change direction and change intensity.

From 1993 to 2000, 213 km^2 of DG was either reversed or significantly reversed annually; 129 km^2 of DG was developed, significantly developed or changed into DG from another land type annually. The spatial dynamic-change intensity of

TABLE IV
GRASSLAND SANDY DESERTIFICATION DEVELOPMENT TENDENCY OF THE STUDY AREA OVER DIFFERENT PERIODS

	1993–2000		2000–2006		2006–2011	
	Area (km^2)	Proportion (%)	Area (km^2)	Proportion (%)	Area (km^2)	Proportion (%)
Seriously developed	172	2.54	110	1.62	121	1.79
Developed	734	10.84	469	6.92	864	12.75
Stable	4376	64.60	4232	62.47	4672	68.97
Reversed	1056	15.59	1421	20.97	952	14.05
Significantly reversed	436	6.44	543	8.02	165	2.44

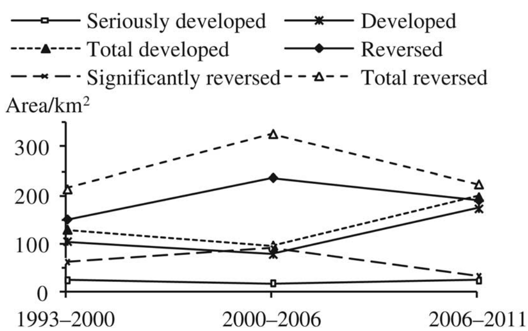

Fig. 5. Grassland desertification spatial distribution dynamic-change intensity tendency chart for Yanchi County.

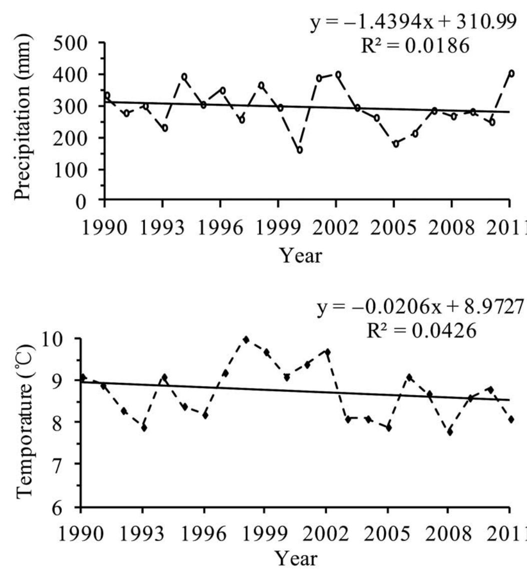

Fig. 6. Change in annual precipitation and temperature in Yanchi County from 1990 to 2011.

the grassland desertification shows that the reversion is greater than the development, and the gap between them increased during 2000–2006: the total area in which desertification developed annually was only 96 km^2 but the total area in which it was reversed was 327 km^2. This indicates that the progress of grassland desertification has been efficiently controlled. Then, during the period 2006–2011, the gap between the annual total reversed and total developed areas significantly narrowed.

C. Discussion

The distribution of the Mu Us Sandland inside Yanchi County provides the material basis for the formation and development of desertification. In 2009, research by Xu *et al.* [37] showed that grassland desertification occurs mainly in the topsoil (0–20 cm deep) in Yanchi County. In terms of material composition, the Sandland consists of sand particles, with lower proportions of powder clay and clay. A soil structure like this is susceptible to the influence of outside intervention; however, the xerophytes, widely distributed in the territory of Yanchi County, will grow fast if there is no detrimental effect, and then play a role in windbreaks and sand fixation.

The evolution of the ecological environment substantially reflects both natural and human factors. Natural factors, such as precipitation and temperature, are important influences on the growth of grassland vegetation. The average annual temperature has fluctuated in a downward trend since 1990 (Fig. 6), which has helped to reduce evapotranspiration, maintain soil moisture and provide favorable conditions for vegetation growth. Yanchi County is located in the transition zone between the arid and the semiarid zone, where precipitation is the limiting factor in the growth and development of the natural vegetation. Between 1990 and 2011, the annual precipitation was also in a fluctuating downward trend, which would affect the growth of vegetation, especially in MDG and SeDG areas with poor water-holding capacity and low levels of soil nutrients. As precipitation is the only source of water, a reduction seriously affects the growth of vegetation in these areas, which reduces the capacity for windbreaks and sand fixation, which can impede the process of desertification reversal and allow further development of desertification.

In spite of the overall trend of precipitation and other factors are not conducive to the reversion of grassland desertification in the monitoring period in Yanchi County, development and utilization of land resources have been cautiously positive with an increase in population and economic development. Facing the worsening desertification process, China has made great efforts to combat desertification and implement the United Nations Convention to Combat Desertification (UNCCD). Besides enacting the Law of Combating Desertification and the National Plan for Combating Desertification, China also launched a series of key national ecological projects, such as the Three-North Shelterbelt Project (1978–present), Beijing and Tianjin Sandstorm Source Treatment Project (2001–2010), the Cropland Conversion Project (2003–present), and the Pastureland Conversion Project (2003–present). Some local governments implemented financial subsidies and some supported policies to push forward desertification control. For example, Ningxia Hui Autonomous Region was the first in China to implement a region-wide grazing ban [38]. As vegetation is no longer being trampled and eaten by livestock following the grazing ban, the cessation of destruction from grazing activities has assisted the restoration of grassland vegetation.

Although the implementation of ecological protection has many advantages, if there are no corresponding economic compensation measures and effective guidance for the adjustment of industrial structure, there will inevitably be contradictions between ecological policy and the economic interests of farmers and herdsmen. Research has shown that with the implementation of the grazing ban and the Cropland Conversion Project, among other ecological engineering projects, animal husbandry costs increased and the transfer of surplus labor has been a problem. Yearly per capita income has decreased from 1875.23 yuan in 2004 to 1169.22 yuan in 2011 in Yanchi County [39], suggesting the far-reaching effects of the grazing ban and the importance of animal husbandry to farmers and herdsmen in this region. In addition, compared with the Cropland Conversion Project, financial aid associated with the grazing ban is low and difficult to implement. The implementation of the grazing ban achieved significant results with the strict law enforcement at the beginning, which has been supported by monitoring the results during the period of 2000–2006 in this paper. However, as time went on, the pressure of economic need made it difficult to establish ecological consciousness among the farmers and herdsmen, leading to widespread illegal grazing. A recent study shows that 70% of farmers and herdsmen have grazed without permission [40]. As shown in this paper, compared with the period 2000–2006, the areas of developed and seriously developed grassland desertification significantly increased in the period 2006–2011 and the gap between the total developed and total reversed areas narrowed. Only the combination of ecological protection and action in support of the economic interests of farmers and herdsmen can make ecological protection policy effective.

IV. Conclusion

Monitoring results in this paper show that grassland vegetation is in a recovery state and that the degree of desertification continued to be mitigated over the period from 1993 to 2011. The reduction in desertified grassland was greatest between 2000 and 2006, with an annual loss of SeDG of up to 8.86%. The largest gap between the total developed and total reversed areas occurred during the period 2000–2006, with the total area of desertification reversal being 3.40 times the total area of desertification development. Despite increasing precipitation from 2005, the annual increase in the total area of developed desertification was 94.41 km^2 during 2000–2006, rising to 196.95 km^2 during 2006–2011. Overall, natural environmental fluctuations in the study area have not been large and, in a situation of decreasing rainfall, human factors (such as ecological protection policy) have become a major cause of recent ongoing grassland desertification reversal.

This study demonstrates that satellite data, especially Landsat data, are useful for the long-term retrospective monitoring of environmental change. However, despite our promising results, there are limitations to the accuracy of using Landsat data, and higher-resolution images must be applied. In this study, the application of SMA to Landsat data appeared to be a consistent, accurate, and low-cost technique to obtain more objective information on the vegetation coverage and bare-sand ratios.

Despite iteratively testing with field data, errors caused by the transient nature of remote sensing images are unavoidable [41]. In particular, it is difficult to precisely estimate changes in conditions over a period of desertification because of the instantaneity of remote sensing images and the volatility of vegetation growth status caused by variations in the precipitation. Improved grassland desertification information extraction methods, further weakening the interference from fluctuations in annual precipitation, as well as building a more efficient, stable, and sensitive grassland desertification assessment indicator system, are the keys to improving the precision of grassland desertification monitoring, and also the future direction of this research.

References

[1] Z. D. Zhu, “Concept, cause and control of desertification in China,” *Quat. Sci.*, vol. 2, pp. 145–155, 1998.

[2] UNCCD, *United Nations Convention to Combat Desertification: In Those Countries Experiencing Serious Drought and/or Desertification, Particularly in Africa*. Geneva, Switzerland: UNEP, 1994.

[3] Development Planning Department of Agriculture, *National Grassland Ecological Construction Planning*. Beijing, China: Agriculture Press, 2002.

[4] T. B. Li, G. J. Zhang, and M. X. Wen, “Causes of soil desertification in the key windy-sandy region in Ningxia,” *J. Northwest Forestry Univ.*, vol. 4, no. 18, pp. 70–73, 2003.

[5] K. L. Jia, Q. R. Chang, and J. H. Zhang, “Spatial-temporal change characteristics of sandy desertified lands in agro-pasture interlacing zone in northern Shaanxi,” *J. Desert Res.*, vol. 2, no. 29, pp. 223–228, 2009.

[6] J. Y. Li *et al.*, “Dynamic changes and driving force of grassland sandy desertification in Xilin Gol: A case study of Zhenglan Banner,” *Geogr. Res.*, vol. 9, no. 30, pp. 1669–1682, 2011.

[7] X. S. Yu, M. Zhao, F. Z. Chen, and K. Wang, “Dynamic remote sensing monitoring and analysis on desertification in the northern farming-pastoral zone based on GIS—A case of Tongliao, Inner Mongolia,” *J. Arid Land Resour. Environ.*, vol. 4, no. 24, pp. 107–111, 2010.

[8] Z. P. Wang, “Current situation and trend of dynamic change of desertification land in Ningxia,” *Xinjiang Agric. Sci.*, vol. S2, pp. 93–97, 2010.

[9] C. Z. Yan, Y. M. Wang, S. S. Feng, and J. H. Wang, “Macro-scale survey and dynamic studies of sandy land in Ningxia by remote sensing,” *J. Desert Res.*, vol. 2, pp. 34–37, 2003.

[10] L. M. Yu, Z. P. Wang, A. D. Jiang, J. Ren, and Q. B. Li, “Dynamic change trend analysis of Ningxia desertification,” *Ningxia J. Agric. Forestry Sci. Technol.*, vol. 9, pp. 54–56, 2011.

[11] T. Wang, C. Z. Yan, X. Song, and J. L. Xie, “Monitoring recent trends in the area of aeolian desertified land using Landsat images in China’s Xinjiang region,” *ISPRS J. Photogramm. Remote Sens.*, vol. 68, pp. 184–190, 2012.

[12] X. F. Zhang, C. H. Liao, J. Li, and Q. Sun, “Fractional vegetation cover estimation in arid and semi-arid environments using HJ-1 satellite hyperspectral data,” *Int. J. Appl. Earth Observ. Geoinf.*, vol. 21, pp. 506–512, 2013.

[13] S. Sommer *et al.*, “Application of indicator systems for monitoring and assessment of desertification from national to global scales,” *Land Degrad. Dev.*, vol. 2, no. 22, pp. 184–197, 2011.

[14] C. Zucca, R. D. Peruta, R. Salvia, S. Sommer, and M. Cherlet, "Towards a world desertification atlas. Relating and selecting indicators and data sets to represent complex issues," *Ecol. Indic.*, vol. 1, no. 15, pp. 157–170, 2012.

[15] G. Ding, "Study on indicative feature and cover classification of vegetation in regional desertification assessment—Taking Mu Us Sandland as an example," *J. Soil Water Conserv.*, vol. 1, no. 18, pp. 158–160, 188, 2004.

[16] S. Gao, B. Wang, L. Zhu, J. Wang, and Y. Zhang, "Monitoring and evaluation indicator system on sandy desertification of China," *Sci. Silvae Sin.*, vol. 2, no. 34, pp. 1–10, 1998.

[17] T. Wang *et al.*, "Spatial-temporal changes of sandy desertified land during last 5 decades in northern China," *Acta Geogr. Sin.*, vol. 2, no. 59, pp. 203–212, 2004.

[18] J. Y. Li *et al.*, "Monitoring and analysis of grassland desertification dynamics using Landsat images in Ningxia, China," *Remote Sens. Environ.*, vol. 138, pp. 19–26, 2013.

[19] M. Dawelbait and F. Morari, "Monitoring desertification in a Savannah region in Sudan using Landsat images and spectral mixture analysis," *J. Arid Environ.*, vol. 80, pp. 45–55, 2012.

[20] M. Dawelbait and F. Morari, "Limits and potentialities of studying dryland vegetation using the optical remote sensing," *Ital. J. Agron.*, vol. 2, no. 3, pp. 97–106, 2010.

[21] K. J. Wessels, F. van den Bergh, and R. J. Scholes, "Limits to detectability of land degradation by trend analysis of vegetation index data," *Remote Sens. Environ.*, vol. 125, pp. 10–22, 2012.

[22] J. Y. Li, *The Research and Application of Methods Used in Grassland Sandy Desertification Monitoring Based on TM Data*. Beijing, China: Chinese Academy of Agricultural Sciences, 2011.

[23] A. J. Elmore, J. F. Mustard, S. J. Manning, and D. B. Lobell, "Quantifying vegetation change in semiarid environments: Precision and accuracy of spectral mixture analysis and the normalized difference vegetation index," *Remote Sens. Environ.*, vol. 1, no. 73, pp. 87–102, 2000.

[24] Z. L. Li *et al.*, "Satellite-derived land surface temperature: Current status and perspectives," *Remote Sens. Environ.*, vol. 131, pp. 14–37, 2013.

[25] Z. L. Li *et al.*, "A review of current methodologies for regional evapotranspiration estimation from remotely sensed data," *Sensors*, vol. 5, no. 9, pp. 3801–3853, 2009.

[26] G. Jiapaer, X. Chen, and A. Bao, "A comparison of methods for estimating fractional vegetation cover in arid regions," *Agric. Forest Meteorol.*, vol. 12, no. 151, pp. 1698–1710, 2011.

[27] G. S. Okin, "Relative spectral mixture analysis—A multitemporal index of total vegetation cover," *Remote Sens. Environ.*, vol. 4, no. 106, pp. 467–479, 2007.

[28] M. A. Goenaga, M. C. Torres-Madronero, M. Velez-Reyes, S. J. Van Bloem, and J. D. Chinea, "Unmixing analysis of a time series of hyperion images over the Guánica dry forest in Puerto Rico," *IEEE J. Sel. Top. Appl. Earth Observ. Remote Sens.*, vol. 6, no. 2, pp. 329–338, Apr. 2013.

[29] A. D. Collado, E. Chuvieco, and A. Camarasa, "Satellite remote sensing analysis to monitor desertification processes in the crop-rangeland boundary of Argentina," *J. Arid Environ.*, vol. 1, no. 52, pp. 121–133, 2002.

[30] J. Yang, P. J. Weisberg, and N. A. Bristow, "Landsat remote sensing approaches for monitoring long-term tree cover dynamics in semi-arid woodlands: Comparison of vegetation indices and spectral mixture analysis," *Remote Sens. Environ.*, vol. 119, pp. 62–71, 2012.

[31] J. E. M. Bioucas-Dias *et al.*, "Hyperspectral unmixing overview: Geometrical, statistical, and sparse regression-based approaches," *IEEE J. Sel. Top. Appl. Earth Observ. Remote Sens.*, vol. 5, no. 2, pp. 354–379, Apr. 2012.

[32] C. Ichoku and A. Karnieli, "A review of mixture modeling techniques for sub-pixel land cover estimation," *Remote Sens. Rev.*, vol. 3–4, no. 13, pp. 161–186, 1996.

[33] J. Franke, D. A. Roberts, K. Halligan, and G. Menz, "Hierarchical multiple endmember spectral mixture analysis (MESMA) of hyperspectral imagery for urban environments," *Remote Sens. Environ.*, vol. 8, no. 113, pp. 1712–1723, 2009.

[34] F. J. Garcia-Haro, S. Sommer, and T. Kemper, "A new tool for variable multiple endmember spectral mixture analysis (VMESMA)," *Int. J. Remote Sens.*, vol. 10, no. 26, pp. 2135–2162, 2005.

[35] H. A. Ghrefat and P. C. Goodell, "Land cover mapping at Alkali Flat and Lake Lucero, White Sands, New Mexico, USA using multi-temporal and multi-spectral remote sensing data," *Int. J. Appl. Earth Observ. Geoinf.*, vol. 4, no. 13, pp. 616–625, 2011.

[36] R. Sonnenschein, T. Kuemmerle, T. Udelhoven, M. Stellmes, and P. Hostert, "Differences in Landsat-based trend analyses in drylands due to the choice of vegetation estimate," *Remote Sens. Environ.*, vol. 6, no. 115, pp. 1408–1420, 2011.

[37] D. M. Xu, C. F. Liu, Y. Z. Xie, and K. Wang, "Changes of soil properties during sandy desertification for grassland in Yanchi county," *Res. Soil Water Conserv.*, vol. 4, no. 16, pp. 85–88, 2009.

[38] W. Huang *et al.*, "Effects of grazing prohibition on grassland coverage: A case study at Yanchi county of Ningxia," *Pratacult. Sci.*, vol. 8, no. 28, pp. 1502–1506, 2011.

[39] Y. H. Liu, L. Wang, Y. G. Wang, and N. P. Song, "Comparison of farmers' main income structure at prohibiting graze pro and after in Yanchi county of Ningxia Hui autonomous region," *Res. Soil Water Conserv.*, vol. 3, no. 14, pp. 355–357, 362, 2007.

[40] J. Chen and Y. L. Su, "Effects of grazing ban on production and livelihood of farmers in farming-pastoral zone: A survey of 80 farmers from four villages in two towns," *Probl. Agric. Econ.*, vol. 6, pp. 73–79, 2008.

[41] Z. L. Li *et al.*, "Land surface emissivity retrieval from satellite data," *Int. J. Remote Sens.*, vol. 9–10, no. 34, pp. 3084–3127, 2013.

Jinya Li received the B.S. degree in geographical information science from Hohai University, Nanjing, China, in 2008, and the M.S. and Ph.D. degrees in agricultural remote sensing from the Institute of Agricultural Resources and Regional Planning, Chinese Academy of Agriculture Sciences, Beijing, China, in 2011 and 2014, respectively.

Currently, he is an Assistant Research Professor with the Research Center for Eco-Environmental Science, Chinese Academy of Sciences. His research interests include models and methods for remote sensing image processing, landscape characteristics and dynamic changes of urban ecosystem, and grassland ecology.

Lina Zhao received the B.S. degree in geographical information science from Hohai University, Nanjing, China, in 2008.

Currently, she is an Assistant Engineer with the State Key Laboratory of Systematic and Evolutionary Botany (LSEB), Institute of Botany, Chinese Academy of Sciences, Beijing, China. Since 2008, she is working on geographic distribution patterns and biodiversity conservations of higher plants in China and applications of IUCN Red List in China. Her research interests include geographic information system, assessment of extinction risk of species, database and data processing.

Bin Xu received the Ph.D. degree in ecology from Lanzhou University, Lanzhou, China, in 1995, and finished the Postdoctoral Fellow from Peking University, Beijing, China, in 1997.

Currently, he is a Professor with the Institute of Agricultural Resources and Regional Planning, Chinese Academy of Agriculture Sciences (CAAS), Beijing, China. He is the Discipline Leader of the Prataculture and the Exceptional Talent of the CAAS. He has published more than 140 papers in international conferences and journals. His research interests include growth of grassland, productivity of grassland, turning green of grassland, desertification of grassland, snow disaster, drought of agriculture by remote sensing monitoring, livestock carrying capacity of pastures, grassland resource assessment, and grassland degradation comprehensive treatment.

Xiuchun Yang received the Ph.D. degree in physical geography from Beijing Normal University, Beijing, China, in 2004.

Currently, she is an Associate Researcher with the Institute of Agricultural Resources and Regional Planning, Chinese Academy of Agricultural Sciences, Beijing, China. Her research interests include grassland remote sensing monitoring, desertification monitoring research, and ecological environment quality assessment.

Yunxiang Jin received the Ph.D. degree in agricultural remote sensing from the Institute of Agricultural Resources and Regional Planning, China Academy of Agriculture Sciences (CAAS), Beijing, China, in 2012, and the M.S. degree in physical geography from Nanjing University, Nanjing, China, in 2009.

Since 2012, he is a Postdoctoral Researcher with the Institute of Agricultural Resources and Regional Planning, CAAS. He has published more than 20 papers in journals and conferences. His research interests include remote sensing, remote sensing applications, environment science, geographic information system, climate change, and spatial analysis techniques.

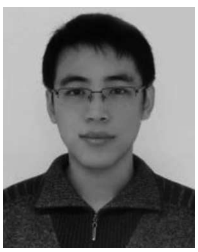

Tian Gao received the Ph.D. degree in agricultural remote sensing from Chinese Academy of Agriculture Sciences, Beijing, China, in 2013.

Currently, he is a Research Associate with the Department of Ecology, Institute of Applied Ecology, Chinese Academy of Sciences, Shenyang, China. His research interests include remote sensing-based vegetation monitor and productivity modeling.

Haida Yu received the B.S. degree in ecology from Agricultural University of Hebei, Baoding, China, in 2010, and the Master's degree in ecology from Chinese Academy of Agricultural Sciences, Beijing, China, in 2013.

Fen Zhao received the B.S. degree in geographical information systems from Liaocheng University, Liaocheng, Shandong, China, in 2011. Currently, she is pursuing the Master's degree at the Institute of Agricultural Resources and Regional Planning, China Academy of Agricultural Science, Beijing, China.

Her research interests include grassland biomass and productivity estimation by remote sensing methods.

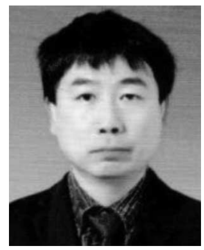

Hailong Ma received the Professional Master's degree in geomatics and natural resource evaluation from the Istituto Agronomico per l'Oltremare (IAO), Florence, Italy, in 2006.

Currently, he is an Assistant Professor with the Institute of Agricultural Resources and Regional Planning, Chinese Academy of Agriculture Sciences (CAAS), Beijing, China. He has published more than 20 papers in international conferences and journals. His research interests include grassland remote sensing, grassland vegetation growth monitoring, and grassland degradation.

Zhihao Qin received the B.Sc. degree in economic geography from Zhongshan University, Canton, China, in 1983, and the Ph.D. degree in remote sensing from Ben Gurion University, Beer Sheva, Israel, in 2000.

Currently, he is a Research Professor with the Institute of Agricultural Resources and Regional Planning, Chinese Academy of Agricultural Sciences, Beijing, China. His research interests include thermal remote sensing and land surface temperature retrieval, remote sensing monitoring of agro-disasters especially agro-drought, impacts of climate change on agriculture, remote sensing and GIS applications to agriculture, and environmental and micrometeorological modeling.